

# Non-linear Simulations of MHD Instabilities in Tokamaks Including Eddy Current Effects and Perspectives for the Extension to Halo Currents

M. Hoelzl<sup>1</sup>, G.T.A. Huijsmans<sup>2</sup>, P. Merkel<sup>1</sup>, C. Atanasiu<sup>3</sup>, K. Lackner<sup>1</sup>, E. Nardon<sup>4</sup>, K. Aleynikova<sup>2</sup>, F. Liu<sup>2</sup>, E. Strumberger<sup>1</sup>, R. McAdams<sup>5,6</sup>, I. Chapman<sup>6</sup>, A. Fil<sup>4</sup>

<sup>1</sup> Max-Planck-Institute for Plasmaphysics, Boltzmannstr. 2, 85748 Garching, Germany

<sup>2</sup> ITER Organisation, Route de Vinon sur Verdon, St-Paul-lez-Durance, France

<sup>3</sup> Association EURATOM-MEdC Romania, P.O. Box MG-36, Magurele, Bucharest, Romania

<sup>4</sup> CEA, IRFM, CEA Cadarache, F-13108 St Paul-lez-Durance, France

<sup>5</sup> York Plasma Institute, University of York, York, YO10 5DD, UK

<sup>6</sup> Culham Science Centre, Abingdon, OX14 3DB, UK

E-mail: mhoelzl@ipp.mpg.de

**Abstract.** The dynamics of large scale plasma instabilities can be strongly influenced by the mutual interaction with currents flowing in conducting vessel structures. Especially eddy currents caused by time-varying magnetic perturbations and halo currents flowing directly from the plasma into the walls are important.

The relevance of a resistive wall model is directly evident for Resistive Wall Modes (RWMs) or Vertical Displacement Events (VDEs). However, also the linear and non-linear properties of most other large-scale instabilities may be influenced significantly by the interaction with currents in conducting structures near the plasma. The understanding of halo currents arising during disruptions and VDEs, which are a serious concern for ITER as they may lead to strong asymmetric forces on vessel structures, could also benefit strongly from these non-linear modeling capabilities.

Modeling the plasma dynamics and its interaction with wall currents requires solving the magneto-hydrodynamic (MHD) equations in realistic toroidal X-point geometry consistently coupled with a model for the vacuum region and the resistive conducting structures. With this in mind, the non-linear finite element MHD code JOREK [1, 2] has been coupled [3] with the resistive wall code STARWALL [4], which allows us to include the effects of eddy currents in 3D conducting structures in non-linear MHD simulations.

This article summarizes the capabilities of the coupled JOREK-STARWALL system and presents benchmark results as well as first applications to non-linear simulations of RWMs, VDEs, disruptions triggered by massive gas injection, and Quiescent H-Mode. As an outlook, the perspectives for extending the model to halo currents are described.

## 1. Introduction

Large scale plasma instabilities can be strongly influenced by the interaction with currents in conducting structures. The resulting forces on wall structures are an important topic for ITER as well. In order to address those questions involving non-linear plasma dynamics and its interaction with wall currents requires a code that solves the magneto-hydrodynamic (MHD) equations in

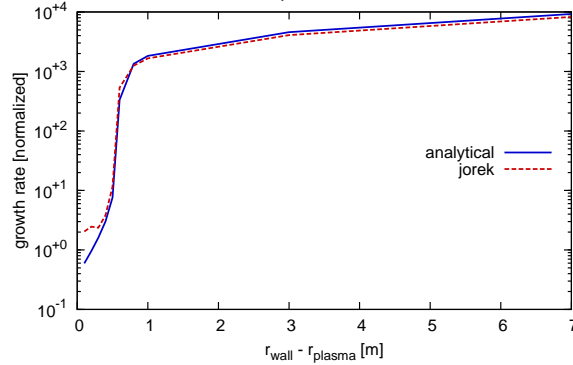


**Figure 1** Comparison of linear growth rates between analytical theory and JOREK-STARWALL results for an RWM case in a circular limiter plasma with minor radius  $a = 1$  m, major radius  $R = 10$  m and at a wall resistivity of  $\eta_{\text{wall}} = 2.5 \cdot 10^{-5} \Omega \text{ m}$ .

realistic toroidal X-point geometry consistently coupled with a model for the vacuum region and the resistive conducting structures. With this in mind, the non-linear finite element MHD code JOREK [1, 2] has been coupled [3] with the resistive wall code STARWALL [4], which allows us to include the effects of eddy currents in 3D conducting structures in non-linear MHD simulations.

This article summarizes the capabilities of the coupled JOREK-STARWALL system (Section 2) and presents benchmark results (Section 3) as well as first physics applications to non-linear simulations (Section 4) of resistive wall modes (RWMs), vertical displacement events (VDEs), disruptions triggered by massive gas injection (MGI), and quiescent H-Mode (QH mode). This publication only provides a brief overview for the physics investigations and refers to separate papers going into more detail on each subject. As an outlook, the perspectives for extending the model to halo currents are described (Section 5).

## 2. The Model

### 2.1. The non-linear MHD code JOREK

The non-linear MHD code JOREK [1] solves a set of reduced MHD equations [5, 6] in realistic toroidal X-point geometry. Two-fluid extensions (diamagnetic drift, separate electron and ion temperatures) and a model for deuterium neutrals exist. A full MHD model is available [7], but needs to be extended by X-point boundary conditions and two-fluid terms.

### 2.2. The resistive wall code STARWALL

The standalone STARWALL code is a resistive wall code [4, 8] capable of linear stability analysis of MHD modes in the presence of 3D resistive walls. Since kinetic energy is neglected, its validity is restricted to cases where plasma inertia does not play an important role. Resistive walls are discretized by triangles using the thin-wall approximation. The validity of this approximation is discussed for instance in Reference [9] and Appendix A.

Parts of STARWALL are currently implemented into the linear MHD code CASTOR [10, 11, 12] along with additional extensions to create the new code CASTOR3D [13] for linear studies including coupling of different toroidal modes by 3D resistive walls, kinetic energy, plasma resistivity and plasma rotation. A modified version of STARWALL (sometimes called STARWALL-J) has been coupled to JOREK to allow non-linear simulations with 3D resistive wall effects. This coupling is described in the following Section.

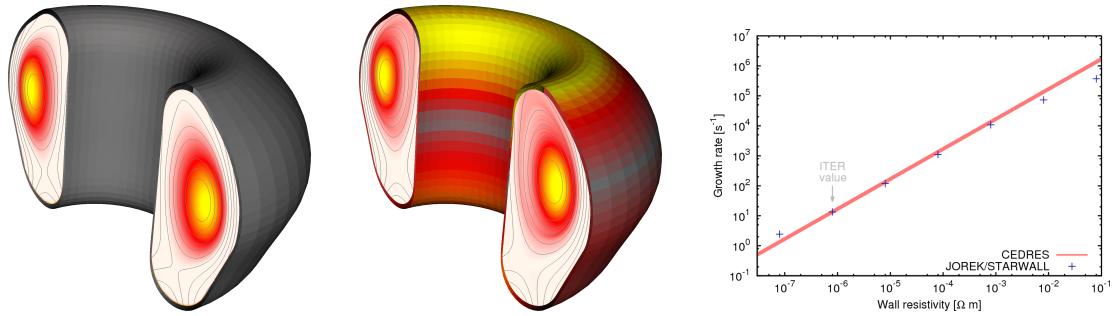


**Figure 2** ITER-like X-point plasma before (left) and during (middle) a VDE with an axisymmetric wall. Colors correspond to the plasma current density (multiplied by  $R$  due to normalization) and wall current density, respectively. The right figure shows the benchmark of linear growth rates for different wall resistivities against the CEDRES++ code with excellent agreement. Small deviations are observed at large wall resistivities since CEDRES++ neglects plasma inertia and at extremely small wall resistivities below the realistic ITER values due to resolution limitations.

### 2.3. The JOREK-STARWALL Coupling

The fully implicit JOREK-STARWALL coupling via a natural boundary condition has already been described previously in detail [3]. This Section only contains a brief summary.

The boundary of the JOREK computational domain is used as “interface” for the coupling of JOREK and STARWALL. STARWALL solves the field equations outside the interface (vacuum region and resistive wall structures) by a variational ansatz with the poloidal magnetic flux  $\psi$  as boundary condition which allows us to obtain an expression for the time evolution of wall currents. STARWALL computes a set of matrices representing this time evolution equation, which are used inside JOREK to keep track of the wall currents.

By considering all possible “unit perturbations”, STARWALL also calculates matrices which allow to express the tangential magnetic field at the JOREK boundary in terms of wall currents and poloidal magnetic flux at the interface. This correlation is used inside JOREK to compute the natural boundary condition – a surface integral in the current definition equation originating from partial integration.

The implementation in JOREK is performed such that the full implicitness of the code is preserved without introducing additional unknowns. To achieve this, the unknown wall currents at time step  $n + 1$  are expressed in terms of the (as well unknown) JOREK variables at the same time step. The coupling is currently implemented only for the reduced MHD model, where the tangential magnetic field perturbation has no toroidal component. STARWALL and the coupling need to be extended in the future by additional matrices to add this additional component. As the STARWALL representation of wall currents allows only divergence-free surface currents, halo currents can presently not be included. Consequently, simulations are limited to eddy currents.

JOREK-STARWALL has already been benchmarked successfully against analytical theory and linear codes as briefly shown in Section 3. First physics results obtained with JOREK-STARWALL are presented in Section 4. An outlook to the inclusion of halo currents, which will be especially important for disruption simulations, is given in Section 5. In separate projects, extensions to impurity massive gas injection and runaway electrons are currently started such that we will be able to address the most important questions related to disruption physics in the future.

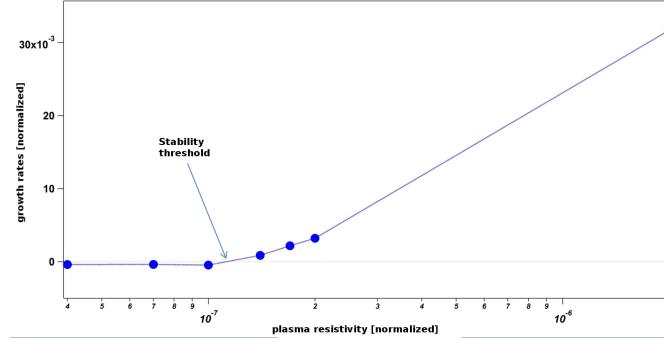


**Figure 3** Simulation of an RWM in ITER geometry, however at artificially increased values of resistivity and viscosity due to computational limitations. The growth rate of the observed instability shows a strong dependence on the plasma resistivity indicating a resistive instability. It is fully stabilized below a threshold in the plasma resistivity. Below this value, stabilizing dissipative effects (like viscosity) become dominant over the growth rate of the resistive instability.

### 3. Benchmarks

This section briefly describes benchmarks carried out for the validation of JOREK-STARWALL. Linear growth rates are compared for resistive wall modes against analytical theory, and for a vertical displacement event against the CEDRES++ code [14]. Additional tests have been carried out earlier [3] by reproducing free-boundary equilibria and comparing tearing mode simulations against a linear code.

#### 3.1. Resistive Wall Modes (RWMs)

The growth rates of a resistive wall mode (RWM) are compared [15, 16] to analytical theory [17] for a circular equilibrium. As seen in Figure 1, linear growth rates show very good agreement except for some deviations at small plasma-wall distances. Such cases where the resistive wall decreases the growth rates of the instability to the order of  $1 \text{ s}^{-1}$  or even below are hard to resolve since the natural boundary conditions tend to induce oscillatory behaviour in these cases. We will identify the reasons and improve this in the near future. This problem disappears for larger plasma-wall distances or higher wall resistivities, where growth rates stay higher.

#### 3.2. Vertical Displacement Events (VDEs)

For an ITER-like VDE testcase with an axisymmetric wall, linear growth rates obtained with JOREK-STARWALL are compared in Figure 2 to the CEDRES++ code and show excellent agreement at realistic ITER wall resistivities [18]. For this benchmark, the plasma resistivity needs to be chosen between an upper limit above which the equilibrium changes too quickly, since we did not use a current source term, and a lower limit below which eddy currents in the scrape off layer would become dominant compared to the resistive wall currents.

### 4. Current Physics Applications

This Section briefly presents first physics applications of JOREK-STARWALL to RWMs, VDEs, QH-Mode, and disruptions triggered by massive gas injection.

#### 4.1. Resistive Wall Modes (RWMs)

Resistive wall modes were simulated in an ITER scenario with reversed q-profile [16]. Results with the realistic location of the conducting wall in ITER were compared to an artificial case with closer wall, and the no-wall case. The comparison of those cases, and additional wall resistivity

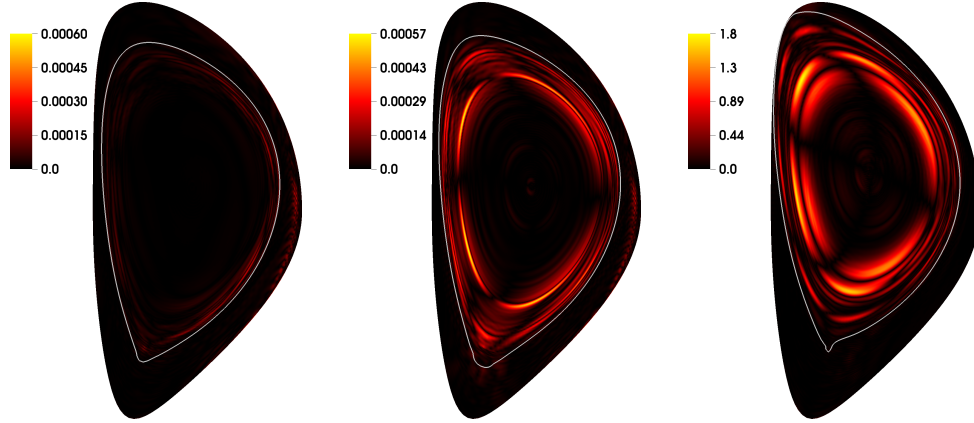


**Figure 4** The absolute value of the  $n = 1$  component of the current density is plotted (in normalized units) close to the beginning of the simulation where the instability is almost axisymmetric (left,  $t = 40 t_A$ ), around the onset of the  $n = 1$  perturbation where the axis has already moved upwards by about 1 cm due to the vertical instability (middle,  $t = 1200 t_A$ ) and at a later stage where the vertical axis displacement is about 32 cm (right,  $t = 9600 t_A$ ). The grey contour line corresponds to the pedestal temperature indicating the location of the separatrix. Clearly, the plasma has changed its shape in the course of the instability and the evolving  $n = 1$  mode has become much less radially localized.

scans allows us to quantify the stabilizing effect of the walls. Figure 3 shows a threshold observed in the plasma resistivity, below which the mode is fully stabilized. Consequently, this mode is a resistive mode. The existence of the threshold and the resistivity value it is observed at depend on the considered equilibrium, wall configuration, and plasma parameters.

#### 4.2. Vertical Displacement Events (VDEs)

A vertical displacement event is an axisymmetric instability where the whole plasma moves up- or downwards with an approximately exponential evolution of the displacement in time. The time scale is governed by geometry and conductivity of conducting structures. A non-axisymmetric component can arise during the non-linear evolution of the VDE (external kink) when the plasma begins to shrink and the  $q$ -profile changes. Figure 4 shows a simulation of a VDE in ITER geometry (however with increased wall and plasma resistivities) which develops such a non-axisymmetric feature [19]. The vertical upward movement of the initially axisymmetric plasma is triggered by a small perturbation of coil currents. A small  $n = 1$  perturbation at the separatrix can be observed (left Figure). A bit later, a  $2/1$  mode sets in at the  $q = 2$  surface while some perturbations between this surface and the separatrix are still visible (middle). The  $2/1$  mode continues to grow and gets radially less localized while the vertical movement of the plasma continues (right).

#### 4.3. Quiescent H-Mode (QH-Mode)

Quiescent H-Mode has been obtained in DIII-D [20], ASDEX Upgrade [21] and other devices. It is characterized by a saturated kink/peeling mode [22] and does not feature periodic ELM crashes. The influence of the vacuum vessel wall on the destabilization and saturation of edge modes for DIII-D QH-mode plasma has been studied with JOREK-STARWALL. Figure 5 shows the flux perturbation and the wall current stream function in the saturated state. When comparing to a fixed boundary simulation (i.e., ideal wall at the JOREK boundary; see Fig. 5 left) the saturated amplitude of the kink/peeling mode is larger in the “free boundary” simulation

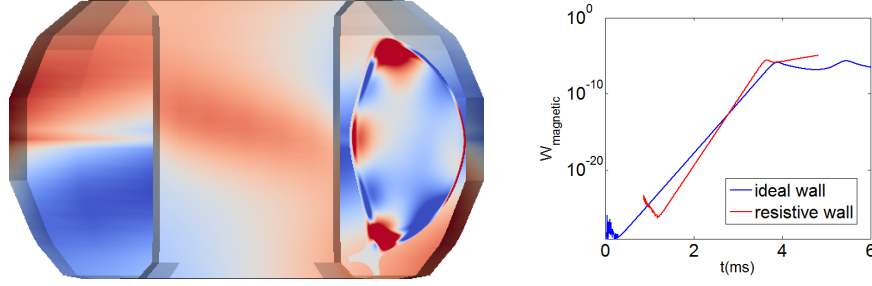


**Figure 5** The perturbed flux and wall potential on the resistive wall are plotted for a saturated kink/peeling mode for a simulation of DIII-D shot #153440 (left) with JOREK-STARWALL. The time evolution of the  $n = 1$  magnetic energy (right) shows that the mode goes into a saturated state. Both, the initial growth rate as well as the saturation level are higher with the resistive wall boundary conditions of JOREK-STARWALL compared to ideal wall boundary conditions at the boundary of the JOREK computational domain.

(resistive wall outside the JOREK domain; see Fig. 5 left). The initially rotating mode gets locked to the wall in the saturated phase of those simulations. To reproduce experimental observations in more detail, toroidal rotation needs to be taken into account (partly done already in Reference [23]), and also effects from neoclassical poloidal and diamagnetic rotation are important (simulations in preparation).

#### 4.4. Disruption Events

JOREK simulations of disruption mitigation by Massive Gas Injection (MGI) are in progress [24]. The focus at the moment is on the cooling phase (when the gas enters the plasma and generates a cold front progressing from the edge to the core) and the triggering and development of the thermal quench (TQ). The MGI is modeled as a poloidally localized (and due to the low toroidal resolution of our first simulations toroidally weakly localized) source of neutrals which are assumed to move only by diffusive processes. Simulations with JOREK standalone (without STARWALL) for a JET plasma showed that an  $m=2$ ,  $n=1$  mode is triggered when the cold front reaches the  $q=2$  surface, and that the TQ ensues when an  $m=3$ ,  $n=2$  mode is destabilized [24]. These simulations have been repeated with STARWALL (for the  $n=1$  harmonic only). Even though the behavior is qualitatively similar, these simulations show quantitative differences and will allow to study, among other things, the dynamics of the locked mode (LM). Indeed, in JET disruptions, a LM is systematically observed. The LM signal is one of the main elements that can be exploited for disruption prediction [25], hence it is important to understand LM physics and its relation with disruptions. Figure 6 shows synthetic LM signals constructed by post-processing the above-mentioned JOREK simulations for JET with and without STARWALL. The left (resp. right) figure shows the amplitude (resp. phase) of the LM signal, which is defined as the  $n=1$  component of the radial magnetic field at the machine midplane. The TQ sets in at about 7 ms, when the signals appear to be noisy. One can see that the LM amplitude peaks slightly before the TQ, with a similar peak value with and without STARWALL, on the order of 4 mT. Experimentally, the LM amplitude also typically presents a peak, although usually it is slightly after the TQ and its magnitude is smaller, typically 0.5...2 mT [De Vries EPS 2014]. The LM phase shows a different behavior with and without STARWALL, probably due to the modified torque exerted by the resistive wall on the plasma. These first MGI simulations do not pretend to be quantitatively correct, for several reasons: only  $n = 0 \dots 2$  harmonics are treated, the atomic physics is simplified, the neutral source is constant in time instead of having a realistic shape, etc. Present work is dedicated to improving all these points in order to simulate

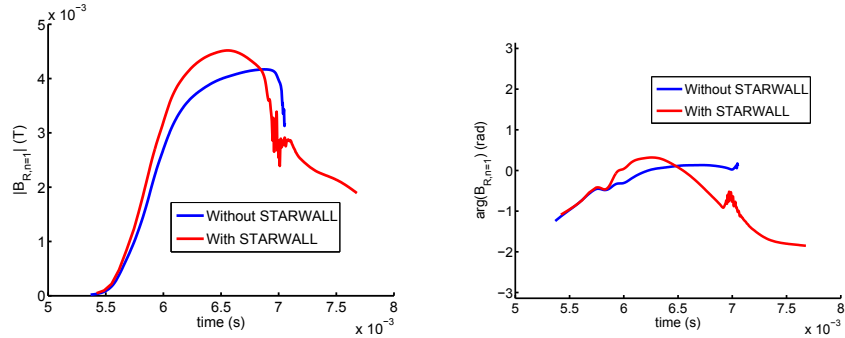


**Figure 6** Amplitude (left) and phase (right) of the synthetic locked mode signal produced as a post-processing of JOREK simulations of MGI in JET. In our simulations, the massive gas injection (currently assuming a neutral source at zero momentum) probably is the main cause for the locking of the MHD activity, since the electro-magnetic force responsible for mode locking vanishes in the ideal wall case.

as realistically as possible a discharge with a D<sub>2</sub> MGI in JET, and to compare the results with experimental measurements in order to validate the model. JOREK-STARWALL will also be essential to study current quench and VDE phases.

## 5. Perspectives for an Extension to Halo Currents

Halo currents arising during a disruption event are a major concern for ITER due to the strong rotating asymmetric forces acting on vessel structures they may cause. Non-linear modeling will be important to predict these forces and also the effectiveness of disruption mitigation techniques aiming to reduce them. The JOREK-STARWALL code, however, currently assumes the wall surface currents to be divergence free, which allows us to include only eddy current effects. This Section provides a brief outlook to a future extension of JOREK-STARWALL to halo currents which effectively are current sources or sinks for the wall currents.

In the present STARWALL code, wall currents are given by  $\mathbf{j}_w = \hat{n} \times \nabla \phi_w$  where the current stream functions  $\phi_w$  are discretized by values at each triangle node and  $\hat{n}$  denotes the normal vector at each triangle. In order to describe halo currents, which effectively enter as sources and sinks for the wall currents, this expression has to be generalized [26] to

$$\mathbf{j}_w = \hat{n} \times \nabla \phi_w + \nabla \varphi_w,$$

by adding a second non-divergence free surface current component, where  $\varphi_w$  takes the role of the electric potential on the wall.

In the derivation of the STARWALL equations, the starting point is a Lagrangian describing the energy associated to the vacuum fields and wall currents which involves terms depending on virtual surface currents (representing the plasma side) and the poloidal magnetic flux at the boundary of the JOREK domain as well as terms depending on the wall currents. A set of time evolution equations can be obtained by applying a variational principle and eliminating the virtual surface currents from the system. The coefficients of the equations can be written in terms of matrices (see Ref. [3]) and are used in JOREK to evolve the wall currents in time. The generalization of the wall current expression will extend the system of equations, i.e., introduce additional matrices and increase the size of some existing matrices. To make further required extensions clear, let us briefly summarize some technical details of the JOREK-STARWALL coupling:

- (i) The JOREK computational grid is constructed and the information describing the boundary of the computational domain is written out, i.e., the boundary nodes and elements.

- (ii) STARWALL calculates the "vacuum + wall response" matrices based on this JOREK boundary information and the desired wall geometry. Another JOREK simulation with a different computational grid requires a new STARWALL run.
- (iii) The JOREK time evolution is carried out in free boundary mode using the STARWALL response matrices to evolve wall currents and to calculate the tangential magnetic field at the boundary of the JOREK domain. The tangential field is required for a boundary integral in the current definition equation arising from partial integration which acts as a natural boundary condition [3].

When introducing halo currents, consistency needs to be guaranteed between plasma and wall for currents flowing between both (current conservation). Additionally, the electric potential must be consistent between plasma and walls. In practice, STARWALL will provide a matrix correlation between currents flowing into the wall and electric potential. This correlation will be used as a boundary condition in JOREK. Although the reduced MHD model of JOREK only has a variable for the toroidal current density, the full current density can be reconstructed (Appendix B) such that halo currents will be compatible with, both, reduced and full MHD models.

A different longer term option would be to implement 3D conducting walls with finite thickness directly into the JOREK domain. A planned future implementation of toroidal finite elements in JOREK (instead of the present toroidal Fourier expansion) will clear the way for this option. STARWALL would then be used for free boundary conditions and conducting structures further away from the plasma. This approach will be tested soon by first implementing an axisymmetric conducting wall inside the JOREK domain.

## 6. Summary

We have presented some benchmarks of the coupled non-linear MHD code JOREK and the resistive wall code STARWALL against linear codes and analytical theory. Some first physics applications to RWMs, VDEs, QH-mode and disruptions were also shown.

An outlook is given to a future extension of JOREK-STARWALL to include halo currents. This will, together with separate other ongoing physics development projects in JOREK, allow for non-linear simulations of the most important processes relevant for disruption physics in the future.

## Acknowledgements

This work was carried out using the HELIOS supercomputer system at Computational Simulation Centre of International Fusion Energy Research Centre (IFERC-CSC), Aomori, Japan, under the Broader Approach collaboration between Euratom and Japan, implemented by Fusion for Energy and JAEA.

## References

- [1] Huysmans G and Czarny O 2007 *Nuclear Fusion* **47** 659
- [2] Czarny O and Huysmans G 2008 *Journal of Computational Physics* **227** 7423 – 7445
- [3] Hoelzl M, Merkel P, Huysmans G, Nardon E, Strumberger E, McAdams R, Chapman I, Günter S and Lackner K 2012 *Journal of Physics: Conference Series* **401** 012010
- [4] Merkel P and Sempf M 2006 *Proceedings of the 21st IAEA Fusion Energy Conference* (Chengdu, China) TH/P3-8 URL [www-naweb.iaea.org/napc/physics/FEC/FEC2006/papers/th\\_p3-8.pdf](http://www-naweb.iaea.org/napc/physics/FEC/FEC2006/papers/th_p3-8.pdf)
- [5] Strauss H 1997 *Journal of Plasma Physics* **57** 83–87
- [6] Franck E, Hoelzl M, Lessig A and Sonnendrücker E *Mathematical Models and Methods in Applied Sciences* In preparation
- [7] Haverkort J 2013 *Magnetohydrodynamic Waves and Instabilities in Rotating Tokamak Plasmas* Ph.D. thesis Eindhoven University of Technology, The Netherlands URL <http://oai.cwi.nl/oai/asset/21317/21317B.pdf>

- [8] Merkel P and Strumberger E MHD stability studies with the STARWALL code in preparation
- [9] Gimblett C 1986 *Nuclear Fusion* **26** 617–625 ISSN 0029-5515
- [10] Huysmans G, Goedbloed J and Kerner W 1993 *Phys. Fluids B* **5** 1545
- [11] Kerner W, Goedbloed J, Huysmans G, Poedts S and Schwarz E 1998 *Journal of Computational Physics* **142** 271 – 303
- [12] Strumberger E, Merkel P, Tichmann C, and Günter S 2011 *Proceedings of the 38th EPS Conference on Plasma Physics* (Strasbourg, France) p5.082
- [13] Strumberger E, Günter S, Merkel P and Tichmann C *Journal of Physics: Conference Series* Submitted
- [14] Hertout P, Boulbe C, Nardon E, Blum J, Brémond S, Bucalossi J, Faugeras B, Grandgirard V and Moreau P 2011” *Fusion Engineering and Design* **86** 1045–1048 Proceedings of the 26th Symposium of Fusion Technology (SOFT-26)
- [15] McAdams R, Chapman I, Wilson H, Hölzl M, Huysmans G, Liu Y and Merkel P 2013 (55th APS Conference)
- [16] McAdams R 2014 *Non-linear Magnetohydrodynamic Instabilities in Advanced Tokamak Plasmas* Ph.D. thesis University of York
- [17] Liu Y, Albanese R, Portone A, Rubinacci G and Villone F 2008 *Physics of Plasmas* **15** 072516
- [18] Hoelzl M, Krebs I, Lessig A, Lackner K, Günter S, Merkel P, Wenninger R, Huysmans G, Nardon E, Orain F and ASDEX Upgrade Team 2013 (15th European Fusion Theory Conference (EFTC), Oxford, UK)
- [19] Aleynikova K and Huijsmans G 2014 Private communication
- [20] Burrell K H, Austin M E, Brennan D P, DeBoo J C, Doyle E J, Gohil P, Greenfield C M, Groebner R J, Lao L L, Luce T C, Makowski M A, McKee G R, Moyer R A, Osborne T H, Porkolab M, Rhodes T L, Rost J C, Schaffer M J, Stallard B W, Strait E J, Wade M R, Wang G, Watkins J G, West W P and Zeng L 2002 *Plasma Physics and Controlled Fusion* **44** A253–A263 ISSN 07413335
- [21] Suttrop W, Hynönen V, Kurki-Suonio T, Lang P, Maraschek M, Neu R, Stäbler A, Conway G, Hacquin S, Kempenaars M, Lomas P, Nave M, Pitts R, Zastrow K D, Team t A U and Workprogramme c t t J E 2005 *Nuclear Fusion* **45** 721–730 ISSN 0029-5515
- [22] Snyder P, Burrell K, Wilson H, Chu M, Fenstermacher M, Leonard A, Moyer R, Osborne T, Umansky M, West W and Xu X 2007 *Nuclear Fusion* **47** 961
- [23] Liu F, Huijsmans G, Loarte A, Garofalo A M, Solomon W M, Snyder P B and Hoelzl M 2014 *Proceedings of the 41st EPS Conference on Plasma Physics* (Berlin, Germany) o5.135
- [24] Fil A, Nardon E, Beyer P, Becoulet M, Dif-Pradalier G, Grandgirard V, Guirlet R, Hoelzl M, Huijsmans G, Latu G, Lehnen M, Loarte A, Orain F, Pamela S, Passeron C, Reux C, Saint-Laurent F, Tamain P and JET EFDA Contributors 2014 *Proceedings of the 41st EPS Conference on Plasma Physics* (Berlin, Germany) p1.045
- [25] de Vries P, Pautasso G, Nardon E, Cahyna P, Gerasimov S, Maraschek M, Lehnen M, Huijsmans G, Hender T and JET EFDA contributors 2014 *Proceedings of the 41st EPS Conference on Plasma Physics* (Berlin, Germany) o5.133
- [26] Atanasiu C and Zakharov L 2013 *Physics of Plasmas* **20** 092506

## Appendix A. Validity of the thin wall approximation

STARWALL uses the thin wall approximation for 3D resistive wall structures. Conductors are discretized by triangles. The resistivity acting on the surface currents under this assumption is  $\eta_{\text{surf}} = \eta/d$  where  $\eta$  is the specific resistivity of the wall material. We will discuss the validity of the thin wall approximation in the following, showing that it is a reasonable model in most situations. For the discussion, we will consider a typical time scale  $\tau$  of the perturbation, which can either be the inverse of its rotation frequency or the inverse of an instability growth rate.

A magnetic field varying on the characteristic time scale  $\tau$  penetrates into a conductor limited to the skin depth  $\delta_{\text{skin}} = \sqrt{2\eta\tau/(2\pi\mu_r\mu_0)}$ , where  $\mu_0$  denotes the vacuum permeability, and  $\mu_r$  the relative permeability. ITER wall structures are mainly built from austenitic steel, and even martensitic components will be deep in the saturated regime due to the large toroidal field, such that  $\mu_r = 1$  can be taken in estimates. For the steel walls ITER will have ( $\eta \approx 10^{-6} \Omega \text{ m}$ ) we obtain  $\delta_{\text{skin}} \approx 0.5\text{m} \cdot \sqrt{\tau[\text{s}]}$ . The characteristic time for a magnetic perturbation to become homogeneous across the  $d = 6\text{cm}$  thick ITER walls is given by  $\tau_{\text{skin}} = (0.06\text{m})^2/(0.5\text{m}^2/\text{s}) = 7\text{ms}$ .

An external kink mode which can fully be stabilized by an ideally conducting wall, but is unstable in the presence of a resistive wall is called a resistive wall mode. Its growth time  $\tau$  is approximately given by the characteristic  $L/R$  time  $\tau_{\text{wall}}$  of the wall structures, which for the ITER conducting vessel is of the order of 200ms. For such a mode with  $\tau \approx \tau_{\text{wall}} \gg \tau_{\text{skin}}$ , the

field is homogeneous across the wall and the thin wall approximation is well justified.

The opposite limit of an instability that is weakly coupled to the walls and can not be stabilized by ideally conducting walls corresponds to  $\tau \ll \tau_{\text{skin}} \ll \tau_{\text{wall}}$ . In this case, the magnetic perturbation can only penetrate into a very thin surface layer of the conductors. In principle, an effective – increased – resistivity needs to be considered for the wall current evolution:  $\eta_{\text{surf,eff}} = \eta/\delta_{\text{skin}}$  instead of  $\eta_{\text{surf}} = \eta/d$ . However, the wall completely shields the magnetic field associated to such a fast mode and effectively acts as an ideally conducting wall – however with little influence on the mode growth. So a correction for the resistivity is not necessary to describe the dynamics of the mode, the thin wall approximation is well justified.

The remaining case would be an instability with  $\tau \approx \tau_{\text{skin}}$  where the magnetic perturbation associated to the mode has partially penetrated through the wall. This situation corresponds to an increased wall resistivity  $\eta_{\text{surf,eff}}$ , which now really has to be taken into account in order to keep the thin wall approximation valid. The non-linear behaviour of an instability might not be obtained fully accurately with the thin-wall approximation in this case. Tokamak instabilities with such growth rates are, however, rather untypical since the wall coupling must be very marginal.

The geometrical simplification by the thin wall only plays a role if the mode wall distance is smaller than the wall thickness. In such an unusual case (e.g., large passive stabilizing loop present in ASDEX Upgrade), conductors can be discretized by several layers of thin walls.

## Appendix B. Halo currents with reduced MHD

In the JOEREK reduced MHD model, only a toroidal current component exists as a variable. Since the boundary of the JOEREK computational domain is axi-symmetric, no currents could enter the walls preventing halo current modeling. However, the full current vector can be reconstructed assuming low pressure at the JOEREK boundary: The momentum conservation equation then turns into  $\mathbf{j} \times \mathbf{B} = 0$ , i.e., the plasma current is parallel to the magnetic field. The current component flowing into the wall is then given by  $j_{\perp} = j\mathbf{b} \cdot \hat{\mathbf{n}}$ , where  $j$  denotes the toroidal current component in JOEREK,  $\mathbf{b} = \mathbf{B}/B$ , and  $\hat{\mathbf{n}}$  is the unit vector perpendicular to the conducting wall.